Differential and total cross sections for top pair and single top production

Nikolaos Kidonakis

Kennesaw State University, Physics #1202, Kennesaw, GA 30144, USA

DOI: http://dx.doi.org/10.3204/DESY-PROC-2012-02/251

I present theoretical results at approximate NNLO from NNLL resummation for top quark production at the LHC and the Tevatron, including new results at 8 TeV LHC energy. Total cross sections are shown for $t\bar{t}$ production, for single top production in the t and s channels and via associated tW production, and for associated tH^- production. Top quark transverse momentum and rapidity distributions in $t\bar{t}$ production are also presented, as well as new results for t-channel single top and single antitop p_T distributions.

1 Introduction

The top quark is a centerpiece of LHC and Tevatron physics, and both $t\bar{t}$ and single top production are being studied. The LO partonic processes for top-antitop pair production are $q\bar{q} \to t\bar{t}$, dominant at the Tevatron, and $gg \to t\bar{t}$, dominant at LHC energies. For single top quark production the partonic channels are the t channel: $qb \to q't$ and $\bar{q}b \to \bar{q}'t$; the s channel: $q\bar{q}' \to \bar{b}t$; and associated tW production: $bg \to tW^-$. A related process is the associated production of a top quark with a charged Higgs, $bg \to tH^-$.

Higher-order QCD corrections are significant for top quark production. Soft-gluon emission corrections are dominant and have been resummed through NNLL accuracy [1, 2]. Approximate NNLO (and even higher-order [3]) differential cross sections have been derived from the expansion of the NNLL resummed result for $t\bar{t}$ [1] and single top [2] production.

There are several different approaches to resummation (for a detailed review see [4]; yet another approach appeared later in [5]). The approach used here is the only NNLL calculation at the differential cross-section level using the standard moment-space resummation in pQCD.

We note that the threshold approximation works very well not only for Tevatron but also for LHC energies because partonic threshold is still important. There is less than 1% difference between NLO approximate and exact cross sections, and this is also true for differential distributions, see the left plot in Fig. 1.

2 $t\bar{t}$ production

We begin with top-antitop pair production [1]. The NNLO approximate $t\bar{t}$ cross section at the Tevatron, with a top quark mass $m_t = 173$ GeV and using MSTW2008 NNLO pdf [6], is $7.08^{+0.00\,+0.36}_{-0.24\,-0.27}$ pb, where the first uncertainty is from scale variation $m_t/2 < \mu < 2m_t$ and the second is from the pdf at 90% C.L.

The $t\bar{t}$ cross section at the LHC at 7 TeV energy is $163^{+7}_{-5} \pm 9$ pb; at 14 TeV it is 920^{+50+33}_{-39-35} pb. The new result for the current 8 TeV LHC energy is

$$\sigma_{t\bar{t}}^{\rm NNLOapprox}(m_t = 173\,{\rm GeV}, 8\,{\rm TeV}) \quad = \quad 234^{+10}_{-7} \pm 12\ {\rm pb}\,.$$

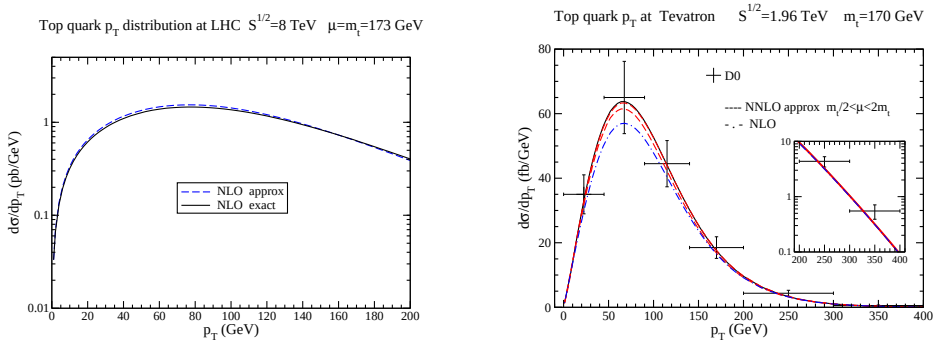

Figure 1: Top quark p_T distribution at the LHC (left) and the Tevatron (right).

The top quark p_T distribution at the Tevatron is shown in the right plot of Fig. 1. We note the excellent agreement of the NNLO approximate results with D0 data [7]. The top quark p_T distributions at the LHC at 7 and 8 TeV energies are shown in the left plot of Fig. 2.

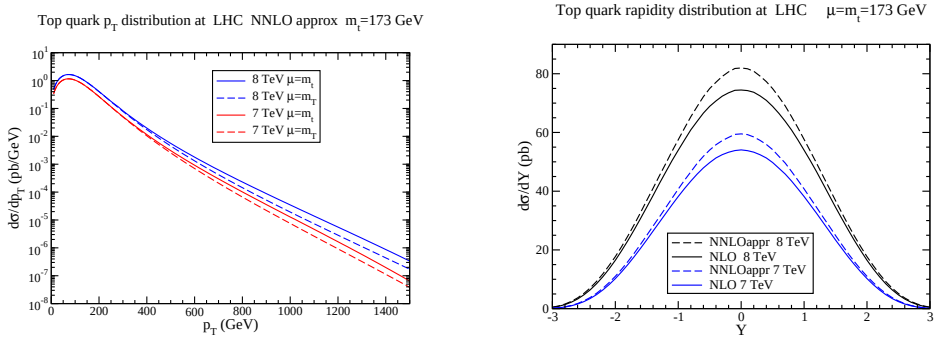

Figure 2: Top quark p_T (left) and rapidity (right) distributions at the LHC [$m_T = \sqrt{p_T^2 + m_t^2}$].

The top quark rapidity distribution at the LHC at 7 and 8 TeV energies is shown in the right plot of Fig. 2. The top quark rapidity distribution at the Tevatron displays a significant forward-backward asymmetry, $A_{\rm FB} = [\sigma(Y > 0) - \sigma(Y < 0)]/[\sigma(Y > 0) + \sigma(Y < 0)] = 0.052^{+0.000}_{-0.006}$, which is smaller than observed values (see also the review in [4] and recently [8, 9]).

3 Single top quark production

We continue with single top production [2], and start with updated results for the t channel.

The t-channel cross sections at LHC energies for single top production, single antitop production, and their sum are given in Table 1. The t-channel single top quark production at the Tevatron is $1.04^{+0.00}_{-0.02} \pm 0.06$ pb; the result for antitop at the Tevatron is the same.

t-channel LHC	t	$\bar{t}$	Total
7 TeV	$43.0^{+1.6}_{-0.2} \pm 0.8$	$22.9 \pm 0.5^{+0.7}_{-0.9}$	$65.9^{+2.1+1.5}_{-0.7-1.7}$
8 TeV	$56.4^{+2.1}_{-0.3} \pm 1.1$	$30.7 \pm 0.7^{+0.9}_{-1.1}$	$87.2^{+2.8+2.0}_{-1.0-2.2}$
14 TeV	$154^{+4}_{-1} \pm 3$	94^{+2+2}_{-1-3}	248^{+6+5}_{-2-6}

Table 1: t-channel cross sections in pb at the LHC for $m_t = 173$ GeV.

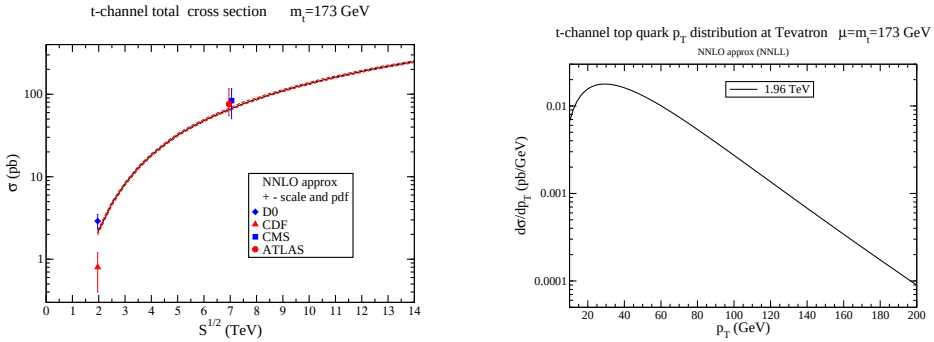

Figure 3: t-channel total cross section versus collider energy (left) and t-channel top quark p_T distribution at the Tevatron (right).

Results for the t-channel total cross section are shown versus collider energy in the left plot of Fig. 3. The right plot of Fig. 3 displays new results for the t-channel top quark p_T distribution at the Tevatron.

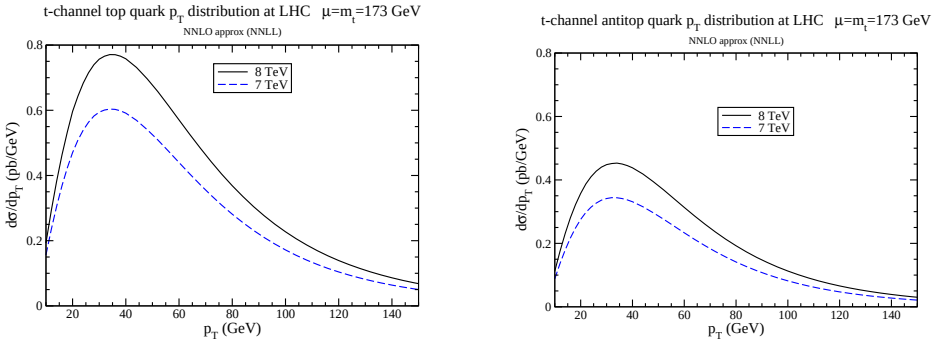

Figure 4: t-channel top (left) and antitop (right) p_T distributions at the LHC.

New results for t-channel top and antitop p_T distributions at the LHC are shown in Fig. 4.

Next we present s-channel results. Table 2 shows the s-channel cross sections at the LHC. The s-channel total cross section versus LHC energy in shown in the left plot of Fig. 5. The s-channel single top cross section at the Tevatron is $0.523^{+0.001+0.030}_{-0.005-0.028}$ pb; the result for antitop production at the Tevatron is identical to that for top.

Next we study the associated tW^- production at the LHC. The tW^- cross section at 7 TeV is $7.8 \pm 0.2^{+0.5}_{-0.6}$ pb; at 8 TeV it is $11.1 \pm 0.3 \pm 0.7$ pb; and at 14 TeV it is $41.8 \pm 1.0^{+1.5}_{-2.4}$ pb.

s-channel LHC	t	$\bar{t}$	Total
7 TeV	$3.14 \pm 0.06^{+0.12}_{-0.10}$	$1.42 \pm 0.01^{+0.06}_{-0.07}$	$4.56 \pm 0.07^{+0.18}_{-0.17}$
8 TeV	$3.79 \pm 0.07 \pm 0.13$	$1.76 \pm 0.01 \pm 0.08$	$5.55 \pm 0.08 \pm 0.21$
14 TeV	$7.87 \pm 0.14^{+0.31}_{-0.28}$	$3.99 \pm 0.05^{+0.14}_{-0.21}$	$11.86 \pm 0.19^{+0.45}_{-0.49}$

Table 2: s-channel cross sections in pb at the LHC for $m_t = 173$ GeV.

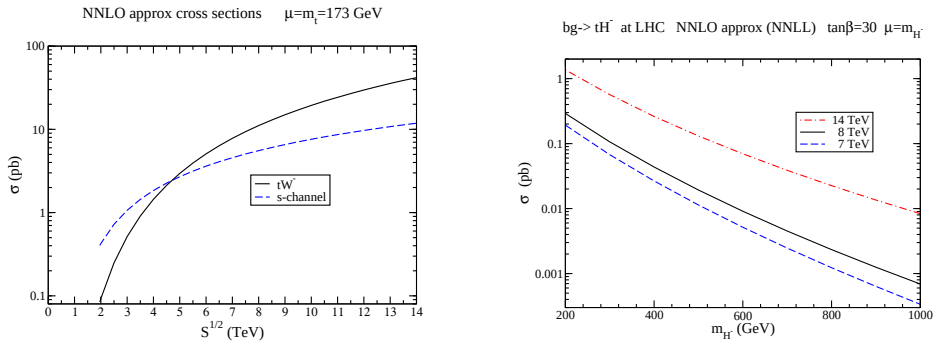

Figure 5: s-channel total and tW^- (left) and tH^- (right) production cross sections.

The cross section for $\bar{t}W^+$ production is identical. The tW^- cross section versus LHC energy in shown in the left plot of Fig. 5.

Finally, we study the associated production of a top quark with a charged Higgs. The right plot of Fig. 5 shows results at LHC energies versus charged Higgs mass with $\tan\beta = 30$.

Acknowledgements

The work of N.K. was supported by the National Science Foundation under Grant No. PHY 0855421.

References

[1] N. Kidonakis. Phys. Rev. **D82** (2010) 114030; Phys. Rev. **D84** (2011) 011504.

[2] N. Kidonakis. Phys. Rev. **D81** (2010) 054028; Phys. Rev. **D82** (2010) 054018; Phys. Rev. **D83** (2011) 091503.

[3] N. Kidonakis. Mod. Phys. Lett. **A19** (2004) 405; Phys. Rev. **D73** (2006) 034001.

[4] N. Kidonakis and B. D. Pecjak. arXiv:1108.6063 [hep-ph].

[5] M. Beneke, P. Falgari, S. Klein, and C. Schwinn. Nucl. Phys. **B855** (2012) 695.

[6] A. D. Martin, W. J. Stirling, R. S. Thorne, and G. Watt. Eur. Phys. J. **C63** (2009) 189.

[7] D0 Collaboration. Phys. Lett. **B693** (2010) 515.

[8] S. J. Brodsky and X.-G. Wu. arXiv:1205.1232 [hep-ph].

[9] P. Skands, B. Webber, and J. Winter. arXiv:1205.1466 [hep-ph].